Organic thin-film transistors based on 2,6-bis(2-arylvinyl)anthracene: high-performance organic semiconductors†

Myoung-Chul Um,[a] Junhyuk Jang,[b] Jung-Pyo Hong,[a] Jihoon Kang,[a] Do Yeung Yoon,[a] Seong Hoon Lee,[a] Jang-Joo Kim*[b] and Jong-In Hong*[a]

Two novel organic semiconductors based on arylvinylanthracene have exhibited good electrical performance (up to 0.2 cm^2 V^{-1} s^{-1}) on OTS treated SiO$_2$/Si at a low substrate deposition temperature and can be easily synthesized in large quantities.

Introduction

Recently, oligothiophene derivatives, linearly fused polycyclic aromatic compounds and their conjugates have been intensively studied due to their potential use as organic semiconductors in various optoelectronic devices, such as organic thin-film transistors (OTFTs), organic light-emitting diodes (OLEDs), photovoltaic cell, sensors, and radio frequency identification (RF-ID) tags.[1–6]

So far, pentacene has shown remarkable properties and is considered the best thin-film material with very high field-effect mobilities. However, pentacene-based devices have poor air stability and rapid device-performance degradation. Although several reports have been published with respect to improving OTFT stability, sufficiently stable organic semiconductors have not yet been realized.

Very recently, several groups have developed semiconductors with high stability and conductivity by choosing conjugated vinylene-based oligomers.[7] In fact, the presence of a double bond of a defined configuration has resulted in a reduction in the overall aromatic character of the planar structures and hence an increase in the π-electron localization. The introduction of a vinylene unit into π-conjugated oligomeric structures is a well-known method for forming coplanar molecules with an extended π-conjugated length, which should help to maximize the organization of the molecules in thin films. The devices derived from vinylene substituted compounds of 2,6-bis[2-(phenyl)vinyl]-anthracene (DPVAnt) not only show very high field-effect mobilities (up to 1.3 cm^2 V^{-1} s^{-1}) and on/off ratios (up to 10^7) but are also found to be exceptionally long-lived and stable in continuous operation under atmospheric conditions.[8] For comparison with other 2,6-bis(2-arylvinyl)anthracenes, DPVAnt devices fabricated in our laboratory under various conditions showed μFET over 1.0 cm^2 V^{-1} s^{-1} and an on/off ratio of > 10^6 under ambient conditions. In addition, OTFT devices derived from 2,6-bis[2-(4-pentylphenyl)vinyl]anthracene (DPPVAnt)

also showed high mobility (0.1–1.28 cm^2 V^{-1} s^{-1}) and on/off ratios (10^6–10^7).[9] However, molecules that incorporate a bigger aromatic group, such as naphthalene and thianaphthene instead of the phenyl group, have not been used as new semiconducting materials for potential high performance, stable OTFTs (Fig. 1). Here we report the synthesis, characterisation and device properties of new semiconductor materials, which have a symmetrically substituted vinylene anthracene backbone with naphthalene and thianaphthene groups.

Experimental

General

^{1}H and ^{13}C NMR spectra were recorded using an Advance 300 MHz Bruker spectrometer in CDCl$_3$. ^{1}H NMR chemical shifts in CDCl$_3$ were referenced to CHCl$_3$ (7.27 ppm), and ^{13}C NMR chemical shifts in CDCl$_3$ were reported relative to CHCl$_3$ (77.23 ppm).

Physical measurement

TGA analyses were performed on a TGA Q50 TA instrument at 10 °C min^{-1} under a nitrogen atmosphere. DSC analyses were performed on a DSC2910 TA instrument at 10 °C min^{-1} under nitrogen flow. UV-Vis absorption spectra were recorded on a BECKMAN COULTER DU 800 spectrophotometer using 2.5 cm path-length quartz cells. For solid-state measurements, oligomers were thermally evaporated in a vacuum chamber on
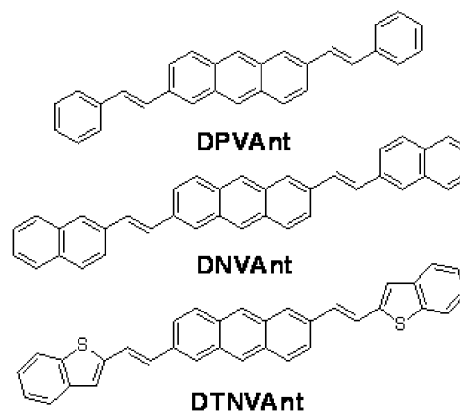
[a] Department of Chemistry, College of Natural Sciences, Seoul National University, Seoul, 151-747, Korea.
E-mail: jihong@snu.ac.kr; Fax: 82-2-889-1568; Tel: 82-2-880-6682
[b] Department of Materials Science and Engineering, Seoul National University, Seoul, 151-744, Korea. E-mail: jjkim@snu.ac.kr; Fax: 82-2-885-9671; Tel: 82-2-880-7085
† Electronic supplementary information (ESI) available: CV, TGA, more detailed device data. See DOI: 10.1039/b803741h

Fig. 1 Structures of DPVAnt, DNVAnt and DTNVAnt.

quartz plates to form 300 Å thick films at a deposition rate of 0.5 Å s^{-1}. XRD analyses were carried out at room temperature with a Mac Science (M18XHF-22) diffractometer using Cu-Kα radiation as the X-ray source at 50 kV and 100 mA. Data were collected in the conventional θ–2θ configuration (2.5–30°) from thin films thermally evaporated in a vacuum chamber on SiO$_2$/Si substrates at 0.5 Å s^{-1} for 300 Å. AFM images of the same vacuum-deposited thin film were taken using a PSIA XE-100 Advanced Scanning Microscope. The voltammetric apparatus used was a CH Instruments model 700 C electrochemical workstation. Cyclic voltammograms (CVs) were obtained at room temperature in a three-electrode cell with a working electrode (Au), a reference electrode (Ag/AgCl), and a counter electrode (Pt) in dichlorobenzene containing tetrabutylammonium hexafluorophosphate (Bu$_4$N$^+$PF$_6^-$, 0.1 M) as a supporting electrolyte at a scan rate of 100 mV s^{-1}. All the potentials were calibrated with the standard ferrocene–ferrocenium redox couple (E = +0.41 V measured).

Fabrication of TFT devices

The field-effect measurements were carried out using top-contact FETs. TFT devices with a channel length (L) of 50 μm and a channel width (W) of 500 μm were fabricated on thermally oxidized, highly n-doped silicon substrates. The SiO$_2$ gate dielectric was 300 nm thick. The organic semiconductor (300 Å) was evaporated (0.1 Å s^{-1} at 1×10^{-6} Torr) onto a non-pretreated or OTS-pretreated oxide surface. Gold source and drain electrodes were evaporated on top of the films through a shadow mask. All measurements were performed at room temperature using a 4155C Agilent semiconductor parameter analyzer, and mobilities (μ) were calculated in the saturation regime by using the relationship: $\mu_{sat} = (2I_{DS}L)/(WC(V_g - V_{th})^2)$, where I_{DS} is the source–drain saturation current; C (1.18×10^{-8} F) the oxide capacitance, V_g the gate voltage, and V_{th} the threshold voltage.

Synthesis

2,6-Bis(chloromethyl)anthraquinone. A mixture of 2.6-dimethylanthraquinone (3.8 g, 16.09 mmol), SO$_2$Cl$_2$ (50 mL), and 2,2′-azobis(2-methyl propionitrile) (0.16 g, 0.96 mmol) was refluxed for 24 h. Excess SO$_2$Cl$_2$ was removed by distillation *in vacuo*. The solid residue was collected by filtration, washed several times with petroleum ether, dried, and recrystallized from DMF to yield 3.8 g (78%) of 2,6-bis(chloromethyl)anthraquinone. ^{1}H NMR (300 MHz, CDCl$_3$): δ 8.41 (m, 4H), 7.98 (s, 2H), 5.00 (s, 4H). High-resolution mass spectrometry (HRMS): Calc. for C$_{16}$H$_{10}$Cl$_2$O$_2$ 304.0057. Found: 304.0034.

2,6-Bis(hydroxymethyl)anthraquinone. A suspension of 2,6-bis(chloromethyl)anthraquinone (3.5 g, 11.47 mmol) in 300 mL of water and 400 mL of DMSO was refluxed with vigorous stirring. Upon heating for 4 h, a clear solution was obtained. The reaction mixture was refluxed for 38 h and then cooled to room temperature. The crystalline product was collected by filtration and recrystallized from DMF to give 3.0 g (98%) of 2,6-bis(hydroxymethyl)anthraquinone. ^{1}H NMR (300 MHz, DMSO): δ 8.17 (m, 4H), 7.85 (d, 2H,

J = 10.7 Hz), 5.57 (s, 2H), 4.70 (s, 4H). High-resolution mass spectrometry (HRMS): Calc. for C$_{16}$H$_{12}$O$_4$ 268.0735. Found: 268.0749.

2,6-Bis(dihydroxymethyl)anthracene. To a solution of 2,6-bis(hydroxymethyl)anthraquinone (2.8 g, 10.43 mmol) in concentrated ammonia (70 mL) was added zinc powder (6.0 g). The reaction was refluxed overnight. The insoluble material was removed by filtration and washed with hot DMSO. The solution was precipitated in 200 mL of 1 M HCl. The product was collected by filtration to give 1.86 g (75%) of 2,6-bis(dihydroxymethyl)anthracene. ^{1}H NMR (300 MHz, DMSO): δ 8.49 (s, 2H), 8.04 (d, 2H, J = 8.7 Hz), 7.94 (s, 2H), 7.46 (d, 2H, J = 8.7 Hz), 5.40 (t, 2H, J = 5.6 Hz), 4.69 (d, 4H, J = 5.6 Hz). High-resolution mass spectrometry (HRMS): Calc. for C$_{16}$H$_{14}$O$_2$ 238.0994. Found: 238.1003.

2,6-Bis(diethylphosphorylmethyl)anthracene. 2,6-Bis(dibromomethyl)anthracene (2.2 g, 6.04 mmol) was added to triethyl phosphite (50 mL), and the resulting solution was refluxed for 12 h. The solvent was removed *in vacuo*, and the residue was purified by column chromatography on silica gel using ethyl acetate–dichloromethane (2 : 1) as the eluent. Yield (90%). ^{1}H NMR (300 MHz, CDCl$_3$): δ 8.35 (s, 2H), 7.97 (d, 2H, J = 8.7 Hz), 7.90 (s, 2H), 7.46 (d, 2H, J = 8.7 Hz), 4.03 (m, 8H), 3.39 (d, 4H, J = 21.8 Hz), 1.26 (t, 12H, J = 7.0). ^{13}C NMR (75 MHz, CDCl$_3$): 131.54, 130.83, 128.75, 128. 61, 128.39, 127. 84, 125. 67, (62.26, 62.16), (35.10, 33.27), (16.44, 16.30). MS (EI) m/z: (M$^+$) Calc. for C$_{24}$H$_{32}$O$_6$P$_2$ 478.16. Found: 478.

2,6-Bis(2-naphthalen-2-yl-vinyl)anthracene (DNVAnt). LDA (1.5 M in cyclohexane, 4.35 mL, 7.83 mmol) was added dropwise to a stirred solution of 2,6-bis(diethylphosphorylmethyl)anthracene (1.5 g, 3.13 mmol) in anhydrous THF (50 mL) at −78 °C under nitrogen. The mixture was stirred for 1 h and then naphthalene-2-carbaldehyde (1.22 g, 7.83 mmol) in THF (10 mL) was added dropwise over a period of 10 min. After the mixture was stirred for 2 h at −78 °C and for 12 h at room temperature, 5 mL of water was added and the solvent was evaporated. The residue was washed with water and MeOH. The desired product was separated by sublimation. High-resolution mass spectrometry (HRMS): Calc. for C$_{38}$H$_{26}$: 482.2034. Found: 482.2032. Anal. Calc.: C, 94.57; H, 4.43. Found: C, 94.66; H, 4.33%.
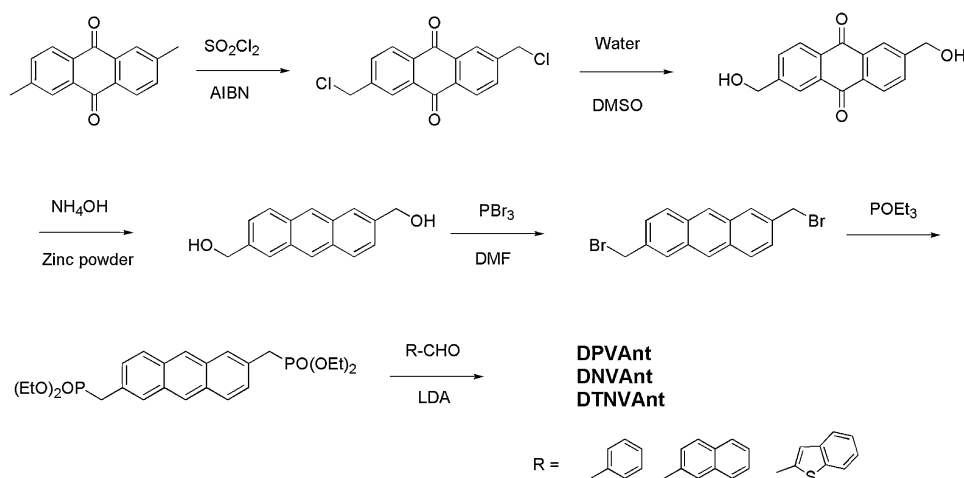
2,6-Bis(2-thianaphtene-2-yl-vinyl)anthracene (DTNVAnt). LDA (1.5 M in cyclohexane, 4.86 mL, 8.76 mmol) was added dropwise to a stirred solution of 2,6-bis(diethylphosphorylmethyl)anthracene (1.4 g, 2.92 mmol) in anhydrous THF (50 mL) at −78 °C under nitrogen. The mixture was stirred for 1 h and then benzo[*b*]thiophene-2-carbaldehyde (1.42 g, 8.76 mmol) in THF (40 mL) was added dropwise over a period of 10 min. After the mixture was stirred for 2 h at −78 °C and for 12 h at room temperature, 5 mL of water was added and the solvent was evaporated. The residue was washed with water and MeOH. The desired product was separated by sublimation. High-resolution mass spectrometry (HRMS): Calc. for C$_{34}$H$_{22}$S$_2$ 494.1163. Found: 494.1162. Anal. Calc.: C, 82.55; H, 4.48; S, 12.96; Found: C, 82.45; H, 4.49; S, 13.03%.
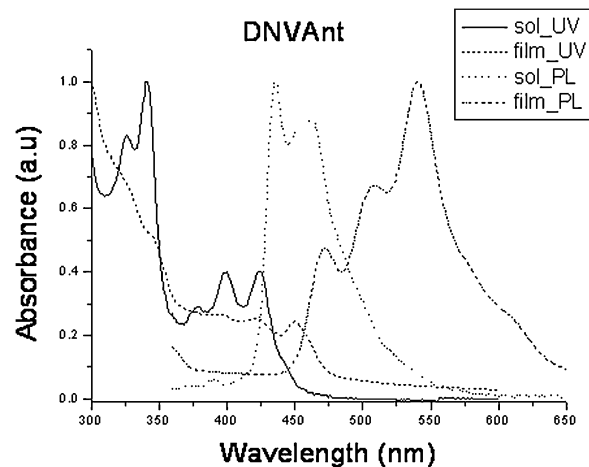
Results and discussion

The synthesis of 2,6-bis-(2-naphthalen-2-yl-vinyl)anthracene (DNVAnt) and 2,6-bis-(2-thianaphtene-2-yl-vinyl)anthracene (DTNVAnt) started from 2,6-dimethylanthraquinone which was prepared from the Diels–Alder reaction of isoprene and p-benzoquinone.[10] Treatment of 2,6-dimethylanthraquinone with an excess of sulfuryl chloride in the presence of a catalytic amount of 2,2′-azobis(2-methylpropionitrile) (AIBN) at refluxing temperature afforded 2,6-bis(chloromethyl)anthraquinone. Refluxing 2,6-bis(chloromethyl)anthraquinone in a mixture of water and DMSO gave the alcohol derivative, which was then reduced with Zn and NH_3 (aq) to give rise to 2,6-bis(hydroxymethyl)anthracene in a good yield. Treatment of the resulting diol with phosphorus tribromide in DMF at room temperature gave 2,6-bis(bromomethyl)anthracene. One of the precursors of the Horner–Emmons olefination, 2,6-bis(diethylphosphorylmethyl)anthracene, was prepared by the reaction of the dibromide with triethylphosphite. The semiconducting materials were synthesized by Horner–Emmons coupling reactions between the phosphonate and aldehyde derivatives, as shown in Scheme 1.

The Horner–Emmons coupling reaction is well known for forming all-*trans* configurations.[11] DNVAnt and DTNVAnt, purified by sublimation, were identified by high-resolution mass spectrometry and elemental analyses.

Two absorption peaks (λ_{max}) were observed for each oligomer. The one at the longer wavelength was around 390–430 nm, corresponding to the π–π* transition of conjugated oligomers, while the shorter wavelength band (λ_{max} 310–350 nm) originated from the electronic transition of the individual aromatic unit. The UV-Vis spectrum of a dilute solution of DNVAnt in xylene showed absorption peaks at 425, 399 and 340 nm, which are similar to the spectra of DTNVAnt (Fig. 2). In general, the absorption spectra were red-shifted with increasing number of acene rings. The long-wavelength absorptions in the films of the two compounds showed slight red-shifts compared to those in solutions (Fig. 2). In general, the absorption spectra were red-shifted with increasing number of acene rings. The long-wavelength absorptions in the films of the two compounds


Fig. 2 Absorption and photoluminescence spectra of DNVAnt in xylene solution and as a thin film.

showed slight red-shifts compared to those in solutions (Fig. S2, ESI†).

Interestingly, in the PL spectra, the differences in emission maxima between the solution and film states of DNVAnt and DTNVAnt are 80 and 110 nm, respectively.[12] This indicates the presence of extremely strong intermolecular interactions in the film states. The HOMO–LUMO energy gaps determined by extrapolating the long-wavelength absorption edge are 2.79 eV for DPVAnt, 2.71 eV for DNVAnt and 2.69 eV for DTNVAnt, significantly higher than that of pentacene (2.2 eV).[13] The lower energy band gaps observed in DNVAnt and DTNVAnt can be attributed to the increase in π conjugation length compared to DPVAnt.

Further insight into the electronic properties of these compounds was provided by cyclic voltammetry (CV). CV measurements of DPVAnt, DNVAnt and DTNVAnt in 0.1 M $Bu_4N^+PF_6^-$–dichlorobenzene solution showed an irreversible oxidation peak. The onset potentials of oxidation were located at 0.76, 0.74 and 0.75 eV vs. ferrocene (FOC). Regarding the energy level of the ferrocene/ferrocenium reference (−4.8 eV), the HOMO energy levels of DNVAnt and DTNVAnt were


Scheme 1 Synthesis of 2,6-bis(2-arylvinyl)anthracene derivatives.
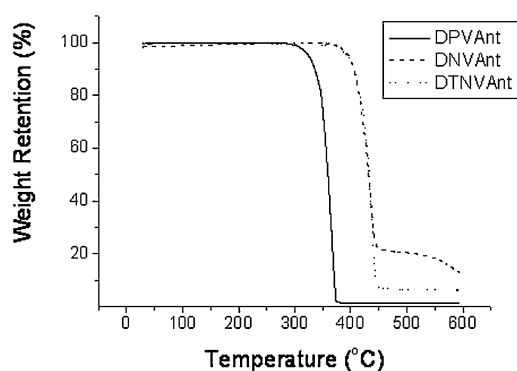
Fig. 3 Thermal gravimetric analysis (TGA) of DPVAnt, DNVAnt and DTNVAnt.

−5.54 and −5.55 eV, respectively (Fig. S6, ESI†).[14] The values of the HOMO level are lower than that of pentacene, thus indicating high oxidative stability.

The thermal stability of DPVAnt, DNVAnt and DTNVAnt were investigated using thermal gravimetric analysis (TGA). Thermal decomposition temperatures were found to be 330 °C for DPVAnt, 394 °C for DNVAnt and 396 °C for DTNVAnt, respectively. Since pentacene began to decompose at 260 °C (due to sublimation), the TGA data indicates that DNVAnt and DTNVAnt compounds are thermally more stable (Fig. 3). Their morphological characteristics were investigated by X-ray diffraction (XRD) (Fig. S3–5, ESI†). The thin-film XRD pattern of DPVAnt displayed a primary diffraction peak at $2\theta = 4.24°$ (d-spacing 20.82 Å), with third- and fourth-order diffraction peaks at $2\theta = 12.08$ and $16.02°$, respectively. The intensity of the X-ray diffraction peaks was strong, indicating the formation of lamellar ordering and crystallinity on the substrate. The d spacing of DPVAnt was estimated to be 20.82 Å from the first reflection peak, which is comparable to the molecular length obtained from the MM2 calculation (22.71 Å). This indicated near-perpendicular alignment of the molecules with respect to the substrate surface. In the thin-film of DNVAnt, sharp reflections up to the fourth order were observed (Fig. S4, ESI†). The d spacing of DNVAnt obtained from the first reflection peak was 25.9 Å, comparable to the molecular length obtained from the MM2 calculation (27.33 Å), suggesting that the molecules are also perpendicular to the substrate surface. On the other hand, the XRD results of DTNVAnt films exhibited weaker reflection peaks than DPVAnt and DNVAnt with the second-order diffraction peak at 6.6°. These films had a rather strong first-order diffraction peak below 3.2°, which was hard to resolve because the incident X-ray was overlapped with the diffracted beam (Fig. S5, ESI†).

The OTFTs of DPVAnt, DNVAnt and DTNVAnt compounds were fabricated using top contact geometry with Au electrodes. Gold source and drain contacts (50 nm) were deposited onto the organic layer through a shadow mask. The channel length (L) and width (W) were 50 and 500 μm, respectively. Thin films of the three conjugated oligomers were formed by vacuum evaporation onto either untreated or octadecyltrichlorosilane (OTS)-coated Si/SiO₂ substrates at various substrate temperatures ($T_{sub} = 25$, 50 and 75 °C).
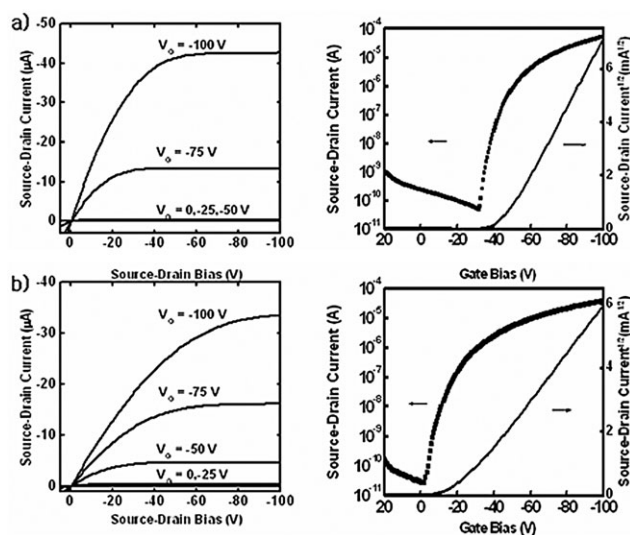
Fig. 4 Source–drain current (I_{DS}) vs. source–drain voltage (V_{DS}) at various gate voltage (V_G) for top-contact field-effect transistor using (a) DNVAnt and (b) DTNVAnt deposited at $T_{sub} = 75$ °C on OTS-treated SiO₂. The transfer characteristics in the saturation regime at a constant source–drain voltage ($V_{DS} = -100$ V) are also included.

All the OTFTs showed typical p-channel TFT characteristics. Fig. 4(a) and (b) show the drain current (I_{DS}) vs. drain-source voltage (V_{DS}), and the transfer characteristics of DNVAnt and DTNVAnt TFTs grown at T_{sub} of 75 °C. From the electrical transfer characteristics, we extracted parameters such as the carrier mobility, on/off current ratio, and threshold voltage for each device. These are summarized in Table 1. The DNVAnt devices fabricated under various conditions showed $\mu_{FET} > 0.1$ cm² V⁻¹ s⁻¹ and an on/off ratio of $>10^5$–10^7 under ambient conditions (Table S1, ESI†). Modification of substrates with a self-assembled monolayer (SAM) of OTS was found to greatly improve the device performance of DPVAnt and DNVAnt. However, the device performance after OTS treatment of DTNVAnt was not significantly improved relative to the unmodified samples (Table S1, ESI†).

In particular, excellent FET characteristics with μFET higher than 0.20 cm² V⁻¹ s⁻¹ (measured in the saturation regime), and an on/off ratio of $>10^7$ were observed in DNVAnt devices fabricated on the OTS-treated substrate at $T_{sub} = 75$ °C (Fig. 4(a)). Fig. 5 shows AFM images of 30 nm thick films of DNVAnt and DTNVAnt deposited onto OTS treated SiO₂/Si at 75 °C. At this temperature, the molecules

Table 1 Field-effect mobility (μ_{TFT}), on/off current ratio (I_{on}/I_{off}), and threshold voltage (V_{th}) of DPVAnt, DNVAnt and DTNVAnt vacuum-deposited on differently treated SiO₂ surfaces and at $T_{sub} = 75$ °C

Compound		T_{sub}/°C	Mobility/ cm² V⁻¹ s⁻¹	I_{on}/I_{off}	Threshold/V_{th}
DPVAnt	OTS	75	1.0	2.2×10^6	−28.9
	Bare	75	0.3	9.0×10^7	−16.2
DNVAnt	OTS	75	0.2	1.1×10^7	−39.2
	Bare	75	0.1	1.3×10^7	−27.3
DTNVAnt	OTS	75	0.1	2.4×10^7	−29.4
	Bare	75	0.1	1.4×10^6	−11.9
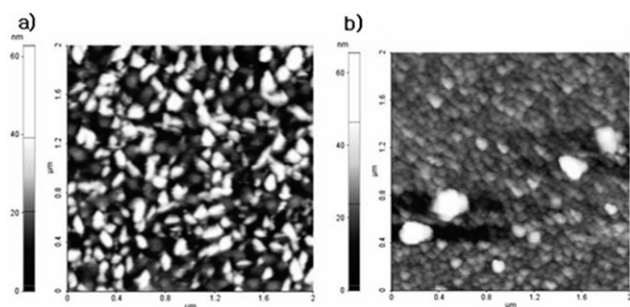
Fig. 5 Nonccontact mode AFM (topography and amplitude) image (2 × 2 um area) of DNVAnt and DTNVAnt at 75 °C; (a) DNVAnt, (b) DTNVAnt.

became more ordered, and a network of interconnected grains was observed for the DNVAnt sample.

Conclusions

We have synthesized two novel organic semiconductors based on arylvinylanthracene, which show good electrical performance (up to 0.2 cm^2 V^{-1} s^{-1}) on OTS treated SiO$_2$/Si and can be easily synthesized in large quantities. In addition, the high mobility of such semiconductors can be achieved at a low substrate deposition temperature. DNVAnt and DTNVAnt show promising properties for applications to organic flexible electronics. We are currently investigating OTFT devices featuring soluble derivatives of DNVAnt and DTNVAnt by the introduction of alkyl chains to DNVAnt and DTNVAnt.

Acknowledgements

References

1 (a) M. H. Yoon, S. A. DiBenedetto, A. Facchetti and T. J. Mark, *J. Am. Chem. Soc.*, 2006, **128**, 9598; (b) K. Takimiya, Y. Kunugi, Y. Konda, H. Ebata, Y. Toyoshima and T. Otsubo, *J. Am. Chem. Soc.*, 2006, **128**, 3044; (c) C. D. Dimitrakopoulos and R. L. Malenfant, *Adv. Mater.*, 2002, **14**, 99.
2 (a) R. H. Friend, R. W. Gymer, A. B. Holmes, J. H. Burrouhes, R. N. Marks, C. Taliani, D. D. C. Bardley, D. A. DosSantos, J. L. Bredas, M. Logdlund and W. R. Salanek, *Nature*, 1999, **397**, 121.
3 (a) C. J. Brabec, N. S. Sariciftci and J. C. Hummelen, *Adv. Funct. Mater.*, 2001, **11**, 15; (b) K. M. Coakley and M. D. McGhee, *Chem. Mater.*, 2004, **16**, 4533.
4 (a) B. Crone, A. Dodabalapur, Y.-Y. Lin, R. W. Filas, Z. Bao, A. LaDu ca, R. Sarpeshkar, H. E. Katz and W. Li, *Nature*, 2000, **403**, 521; (b) Y.-Y. Lin, A. Dodabalapur, R. Sarpeshkar, Z. Bao, W. Li, K. Baldwin, V. R. Raju and H. E. Katz, *Appl. Phys. Lett.*, 1999, **74**, 2714.
5 (a) A. T. Brown, A. Pomp, C. M. Hart and D. M. Deleeuw, *Science*, 1995, **270**, 972; (b) C. J. Drury, C. M. Mutsaers, C. M. Hart, M. Matters and D. M. de Leeuw, *Appl. Phys. Lett.*, 1998, **73**, 108.
6 (a) V. C. Sundar, J. Zaumseil, V. Podzorov, E. Menard, R. L. Willett, T. Someya, M. E. Gershenson and J. A. Rogers, *Science*, 2004, **303**, 1644; (b) V. Podzordov, S. E. Sysoev, E. Loginova, V. M. Pudalov and C. E. Gershenoon, *Appl. Phys. Lett., B*, 2003, **83107**, 3504.
7 (a) C. Videlot-Ackermann, J. Ackermann, H. Brisset, K. Kawamura, N. Yoshimoto, P. Raynal, A. EI Dassmi and F. Fages, *J. Am. Chem. Soc.*, 2005, **127**, 16346; (b) N. Drolet, J. F. Morin, N. Leclerc, S. Wakim, Y. Tao and M. Leclerc, *Adv. Funct. Mater.*, 2005, **15**, 1671; (c) T. C. Gorjanc, I. Levesque and M. D'lori, *Appl. Phys. Lett.*, 2004, **84**, 930.
8 H. Klauk, U. Zschieschang, R. T. Weitz, H. Meng, F. Sun, G. Nunes, D. E. Deys, C. R. Fincher and Z. Xiang, *Adv. Mater.*, 2007, **19**, 3882.
9 H. Meng, F. Sun, M. B. Goldfinger, F. Gao, D. J. Londono, W. J. Marshal, G. S. Blackman, D. D. Dobbs and D. E. Keysa, *J. Am. Chem. Soc.*, 2006, **128**, 9304.
10 H. O. House, J. T. Holt and D. VanDerveer, *J. Org. Chem.*, 1993, **58**, 7516.
11 S. Pfeiffer and H. H. Horhold, *Macromol. Chem. Phys.*, 1998, **200**, 1870.
12 J. H. Park, D. S. Chung, J. W. Park, T. Ahn, H. Kong, Y. K. Jung, J. Lee, M. H. Y. C. E. Park, S. K. Kwon and D. D. Shim, *Org. Lett.*, 2007, **9**, 2573.
13 G. Hill, J. Hwang, A. Kahn, C. Hung and J. E. McDermott, *Appl. Phys. Lett.*, 2007, **90**, 012109.
14 M. S. Liu, Y. Liu, R. C. Urian, H. Ma and A. K.-Y. Jen, *J. Mater. Chem.*, 1999, **9**, 2201.